UNIVERSITÉ PARIS-SACLAY · LICENCE 3 EEA · ELECTRONICS PROJECT, 2025–2026

LiFi Optical Audio Link

First-order Sigma-Delta transmitter and a four-stage analog receiver on a home-made PCB: design, simulation, build and oscilloscope validation

Summary. An audio signal is encoded by a first-order Sigma-Delta (self-oscillating PWM) modulator, sent as on/off light pulses from an LED, and recovered by a receiver made of a photodiode transimpedance amplifier, a conditioning stage, a hysteresis comparator and an active low-pass reconstruction filter. The transmitter self-oscillates at 86.8 kHz with a 52.9 % duty cycle at zero input, and its duty cycle moves to 42.0 % for a +1 V input, a slope of about −1.09 V/V that matches the charge-balance prediction $\langle V_s \rangle = -(R_4/R_3)\langle V_e \rangle$. The receiver was captured in EAGLE, routed on two layers, etched, drilled and soldered by hand, then validated stage by stage at an optical switching rate of about 97 kHz. LTspice simulations show why pulse-width coding survives amplitude noise that a direct analog link cannot reject.

1 · System overview
2 · Transmitter: first-order Sigma-Delta modulator
3 · Simulation: why pulse-width coding resists noise
4 · Receiver: theory and design of the four stages
5 · From schematic to board: PCB design and fabrication
6 · Receiver measurements
7 · Limits and lessons
8 · Conclusion

Team	Mehdi Mechkak, Hamza Dameche, Mangatsa
My part	Receiver: analysis and calculations, EAGLE schematic capture and PCB layout, fabrication, soldering, debugging, oscilloscope characterization of every stage
Given	Transmitter and receiver circuit topologies, encoding strategy and test method were provided by the course instructor
This edition	English rewrite (October 2026) of the original French lab report of 19 May 2026, with corrections listed in Section 7

1 · System overview

LiFi (light fidelity) carries data on light instead of radio waves. The light spectrum is unlicensed and does not interfere with RF systems, but a practical link has to cope with a receiver that sees every photon in the room: the wanted LED pulses arrive mixed with sunlight, ceiling lights and 50/100 Hz mains flicker.

The link studied here keeps the information in the *timing* of the light pulses rather than in their brightness. The transmitter turns the audio into a two-level signal whose duty cycle follows the audio, and drives the LED fully on or fully off. The receiver then only has to answer one question at each instant, "is the LED on?", and averages the answers to rebuild the audio.

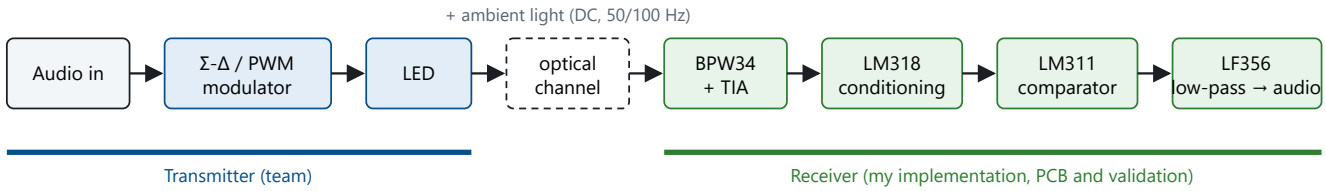


Figure 1. Complete signal chain. Each receiver stage undoes one distortion introduced upstream of it.

The design rests on a frequency separation. Ambient light sits at DC and at low frequencies, audio sits below 20 kHz, and the modulator switches at 85–100 kHz. Because these bands are far apart, the receiver can separate signal from interference with filters instead of needing a strong signal.

1.1 Average value of a two-level signal

For a signal that is $+V_0$ for a fraction α of each period T and $-V_0$ for the rest, the average value is

$$\langle V \rangle = (1/T)\int_0^T V(t)\,dt = V_0\alpha - V_0(1-\alpha) = V_0(2\alpha - 1) \tag{1}$$

A first-order RC low-pass filter with $f_c = 1/(2\pi RC) \ll 1/T$ extracts this average. The spectrum of the signal is a line at DC of height $|\langle V \rangle|$ (zero when $\alpha = 0.5$), the fundamental at $1/T$ and harmonics at n/T whose envelope falls as $1/n$. Recovering the audio means keeping everything below 20 kHz and removing the switching lines.

2 · Transmitter: first-order Sigma-Delta modulator

2.1 Why Sigma-Delta rather than ramp-comparison PWM

Classic PWM compares the audio with a locally generated triangle wave, so any non-linearity of that ramp becomes audio distortion, and quantization noise is spread evenly over frequency. A first-order Sigma-Delta loop avoids both problems. It needs no external ramp because it oscillates on its own, and the integrator in the loop pushes quantization noise towards high frequencies (noise shaping), where the receiver's low-pass filter removes it. The feedback also corrects component non-linearities.

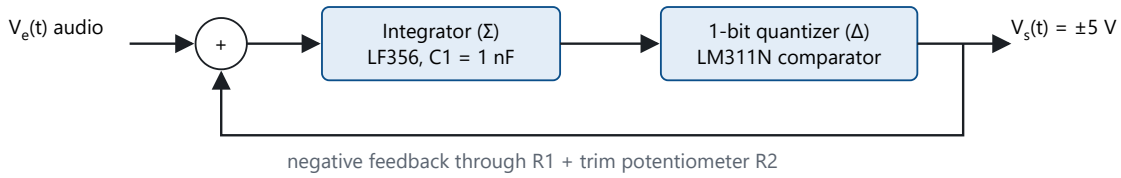


Figure 2. First-order Sigma-Delta loop: the comparator watches the integrated error, not the audio itself.

2.2 Loop equations

At the virtual-ground node of the integrator (bias current neglected), the capacitor current is the sum of the input and feedback currents:

$$i_{C1}(t) = V_e(t)/R_3 + V_s(t)/R_4, \quad dV_a/dt = -(1/C_1)\cdot[V_e/R_3 + V_s/R_4] \tag{2}$$

With V_e constant and $V_s = \pm V_{sat}$, the slope of V_a is constant between switching events, so the integrator output is made of straight ramps. The integrator and the comparator each invert the signal, so the loop is negative feedback at DC. The delay before the comparator switches adds phase shift, and at the frequency where that shift reaches 180° the loop sustains a relaxation oscillation.

Oscillation period (hysteresis version). In the instructor's design the comparator has hysteresis set by a divider R_1, R_2: the thresholds are $\pm V_{th} = \pm V_{sat}\cdot R_1/(R_1+R_2)$. For $V_e = 0$, V_a ramps between the two thresholds in $T/2$, which gives

$$T = 4\cdot V_{th}\cdot R_4C_1/V_{sat} = 4\cdot R_1R_4C_1/(R_1+R_2) \tag{3}$$

The supply voltage cancels: the period depends only on component values. With $R_1 = R_2 = 10$ kΩ and $V_{sat} = \pm 5$ V, the thresholds are ±2.5 V.

Charge balance. In steady state the capacitor cannot charge indefinitely, so the average current through it is zero. Averaging (2):

$$\langle V_e\rangle/R_3 + \langle V_s\rangle/R_4 = 0 \;\Rightarrow\; \langle V_s\rangle = -(R_4/R_3)\cdot\langle V_e\rangle \tag{4}$$

The average of the two-level output is proportional to the input. Combined with (1), the duty cycle carries the audio, and a low-pass filter at the receiver gets it back.

2.3 Components as built

Block	Part	Reason
Integrator	LF356 (JFET input, GBW ≈ 5 MHz, slew rate ≈ 12 V/µs), C1 = 1 nF, input resistors R3 = R6 = 10 kΩ	pA bias current, fast enough to follow ramps at ~100 kHz; a small C1 gives steep ramps and a high oscillation frequency
Quantizer	LM311N, open-collector output, 1 kΩ pull-up to +5 V	dedicated comparator, ~200 ns response, so little extra loop delay
Feedback	R1 + trim potentiometer R2	sets the loop gain R4/R3 and lets the zero-input duty cycle be centred
LED driver	680 Ω series resistor, 47 µF local reservoir capacitor	limits LED current; supplies the switching current peaks without disturbing the analog rails

> **Note on the comparator threshold.** Three versions exist in the project and they are not the same circuit: the instructor's hysteresis design (±2.5 V, equation 3), our LTspice model (whose values give ±1.5 V, Figure 7), and the board we wired, where the LM311N compares the integrator output with 0 V. Without hysteresis, the switching frequency is set by the integrator slope and the propagation delay of the loop rather than by equation (3). That is why we compare the bench results with the charge-balance law (4), which does not depend on the threshold, and not with (3).

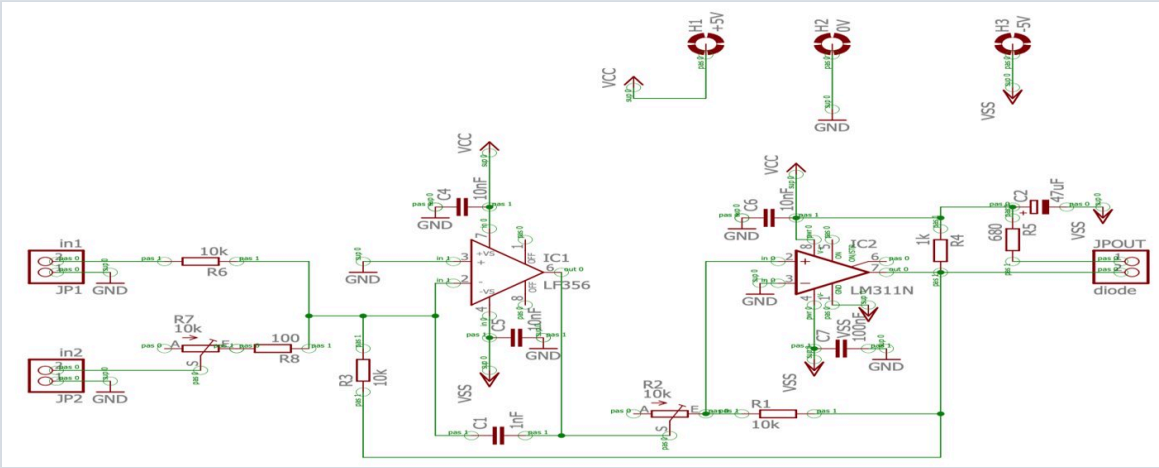


Figure 3. Transmitter schematic (integrator, comparator, LED stage).

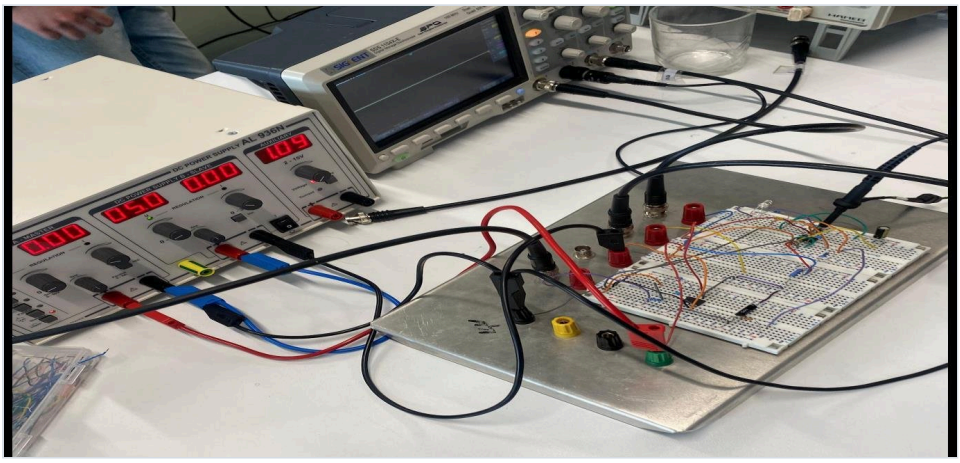


Figure 4. Transmitter on the breadboard, with the ±5 V bench supply and Siglent oscilloscope.

2.4 Bench measurements

The circuit was supplied at ±5 V. The scope shows the comparator output (purple) and the integrator ramps (yellow and blue).

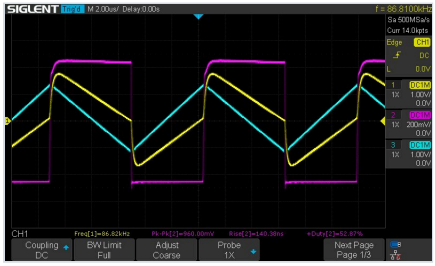


Figure 5a. V_{in} = 0 V: self-oscillation at 86.82 kHz, duty cycle 52.87 %.

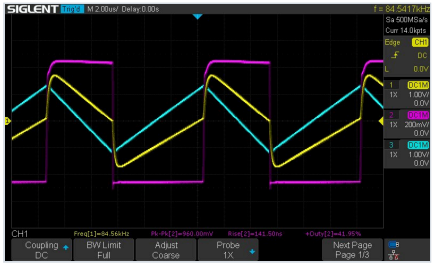


Figure 5b. V_{in} = +1 V DC: 84.56 kHz, duty cycle 41.95 %.

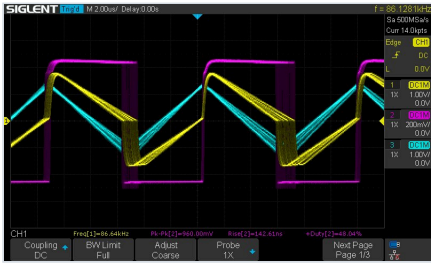


Figure 5c. 1 kHz, 1 V sine input (persistence on): edges sweep with the audio; mean frequency 86.13 kHz.

Test	Frequency	Duty cycle α	$\langle V_s \rangle = 5(2\alpha - 1)$
V_{in} = 0 V	86.82 kHz	52.87 %	+0.29 V
V_{in} = +1 V	84.56 kHz	41.95 %	−0.81 V
1 kHz sine, 1 V	86.13 kHz (mean)	varies with the sine	follows the input

Reading the results. At zero input the loop is nearly balanced. The 2.9-point offset from 50 % corresponds to +0.29 V of output average, which can come from op-amp offset and the slightly asymmetric output levels of the open-collector comparator. A +1 V input moves the output average by −1.09 V, so the measured slope is −1.09 V/V. Equation (4) predicts $-R_4/R_3$, about −1 for equal resistors; the trim potentiometer in the feedback path explains the small difference. The sign is right too: a positive input makes the output spend more time low. With the sine input, the switching frequency stays near 86 kHz, more than four times the top of the audio band. The audio only shifts the edges, which is what the receiver needs.

3 · Simulation: why pulse-width coding resists noise

The modulator and a passive RC demodulator (R5, C2, $f_c = 1/(2\pi R_5 C_2) \approx 1591$ Hz) were simulated in LTspice with a 500 Hz, 1 V test tone.

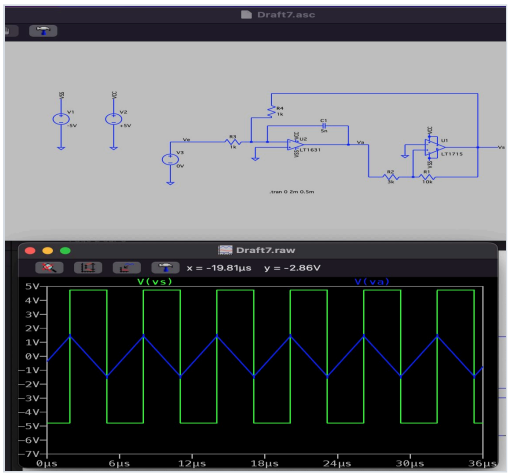


Figure 6. V_e = 0: the integrator output V_a (blue) is a triangle between the comparator thresholds (±1.5 V in this model) and V_s (green) is a ±5 V square wave at 50 % duty.

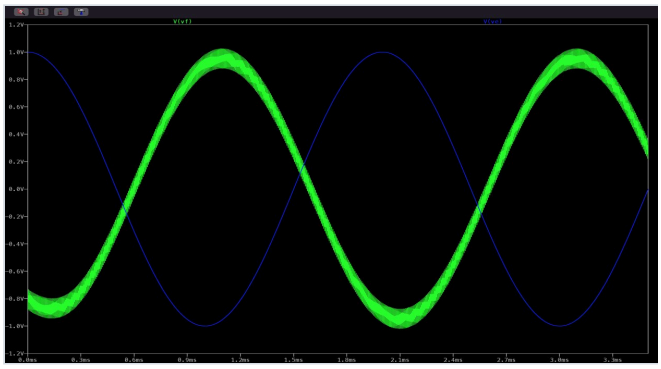


Figure 7. 500 Hz input (blue) and RC-filtered output V_f (green): same frequency, inverted, with a thin residual ripple at the switching rate. The inversion is the minus sign of equation (4).

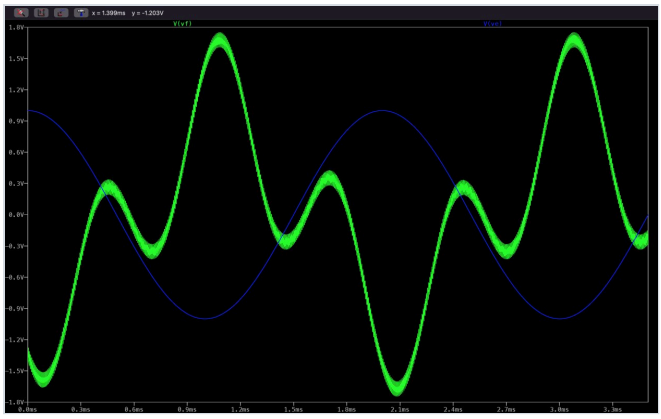


Figure 8. A 1500 Hz disturbance added directly to the transmitted signal and filtered by the same RC: the output is badly distorted, because 1500 Hz lies just under f_c and close to the 500 Hz tone.

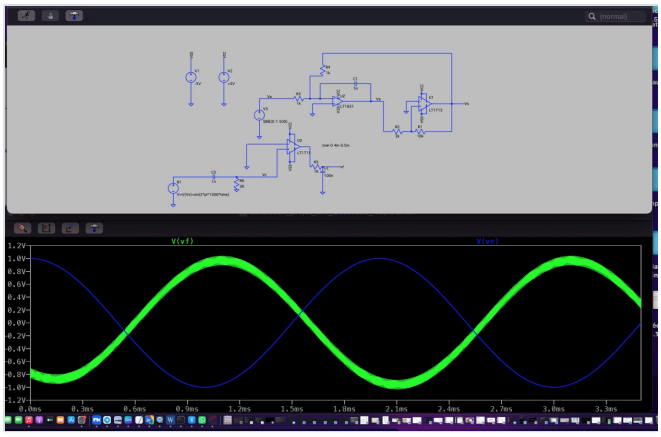


Figure 9. Same disturbance, but with a 0 V comparator before the filter: the clean 500 Hz sine is back.

The difference between Figures 8 and 9 is the main argument for the whole design. In a direct analog link, the 1500 Hz disturbance adds to the amplitude that carries the information, and no simple filter can separate two tones that close. In the PWM link the information is in the switching instants. The disturbance changes the height of the plateaus but barely moves the zero crossings, so a comparator regenerates a perfect two-level signal and the filter sees an undisturbed duty cycle. Driving the LED fully on or off is also more efficient and avoids the non-linear brightness-versus-current curve of the LED.

4 · Receiver: theory and design of the four stages

The photodiode cannot tell an LED photon from a room-light photon, so its current is $I_{ph} = I_{signal}(t) + I_{ambient}$. $I_{ambient}$ is large and mostly DC; I_{signal} is small and sits at the switching frequency. Every choice below (gain, filtering, hysteresis) separates the two by frequency, not by amplitude.

4.1 Stage 1: photodiode and transimpedance amplifier

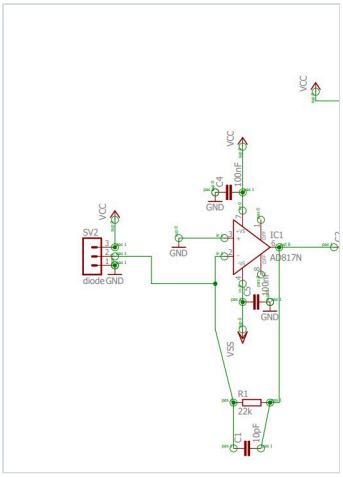


Figure 10. TIA stage (early EAGLE version, op-amp labelled AD817N; the fabricated board uses an LM318): BPW34 into IC1 with R_f = 22 kΩ and C_f = 10 pF.

The BPW34 PIN photodiode feeds the inverting input of IC1, which holds it at virtual ground. Because almost no current enters the op-amp input, the whole photocurrent flows through R_f:

$$V_{TIA} = -R_f \cdot I_{ph} \tag{5}$$

A 10 µA photocurrent gives −0.22 V with R_f = 22 kΩ. A larger R_f would give more signal but also: (1) multiply the ambient DC and push the output towards the rail, (2) lower the bandwidth, (3) reduce phase margin, and (4) add Johnson noise. 22 kΩ is a compromise between these four effects.

Stability. The junction capacitance of the BPW34 (C_j ≈ 72 pF at zero bias, from the datasheet) sits at the inverting input and raises the noise gain at high frequency, which erodes phase margin and can make a bare TIA ring. C_f across R_f compensates this. A common first estimate is

$$C_f \approx \sqrt{(C_{in} / (2\pi \cdot R_f \cdot GBW))} \tag{6}$$

The op-amp changed during the project. An early schematic (Figure 10) used an AD817N and the original French report named an LF356, but the final fabricated board (EAGLE file *recipteur12*) uses an **LM318** for IC1, the same fast op-amp as Stage 2. With the LM318 (GBW ≈ 15 MHz), (6) gives C_f ≈ 5.9 pF; with an LF356 (5 MHz) it would give about 10 pF. The 10 pF fitted on the board is therefore on the safe side for the LM318: more phase margin, with a closed-loop signal bandwidth of $1/(2\pi R_f C_f)$ ≈ 720 kHz, still more than seven times the ~97 kHz switching rate.

4.2 Stage 2: conditioning (LM318)

The TIA output is the PWM signal sitting on a DC offset from ambient light. A low-pass test point lets that offset be measured on its own: with a symmetric 50 % signal the PWM average is zero, so whatever DC remains is ambient light. In the signal path, a high-pass network blocks the ambient component and the LM318 amplifies the remaining AC signal and recentres it around 0 V. The LM318 was chosen for speed (wide bandwidth and high slew rate), so that it can amplify a ~97 kHz square wave without rounding its edges.

A low-pass filter alone cannot remove interference inside the useful band; only a high-pass (or band-pass) can separate slow drift from the wanted high-frequency content.

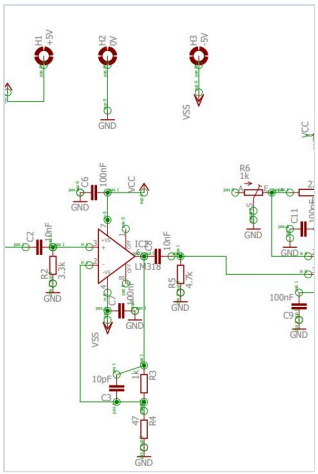
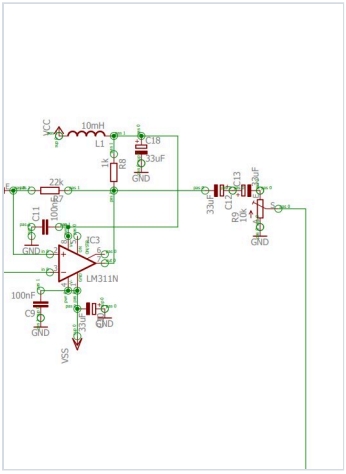


Figure 11. Conditioning stage (EAGLE), IC2 = LM318.

4.3 Stage 3: hysteresis comparator (LM311N)



Driven open-loop, the comparator output jumps to one rail or the other. With a single threshold, noise near the crossing makes it chatter. Positive feedback gives two thresholds, $V_{SH} = +V_{sat}\cdot k$ and $V_{SB} = -V_{sat}\cdot k$, where k is set by the feedback divider. On this board one resistor of the divider is a potentiometer (R6), so the hysteresis window is adjustable and was tuned on the bench. The output is a regenerated two-level signal at about ±5 V that keeps all the timing information.

Figure 12. Comparator stage (EAGLE), IC3 = LM311N.

4.4 Stage 4: reconstruction filter (LF356)

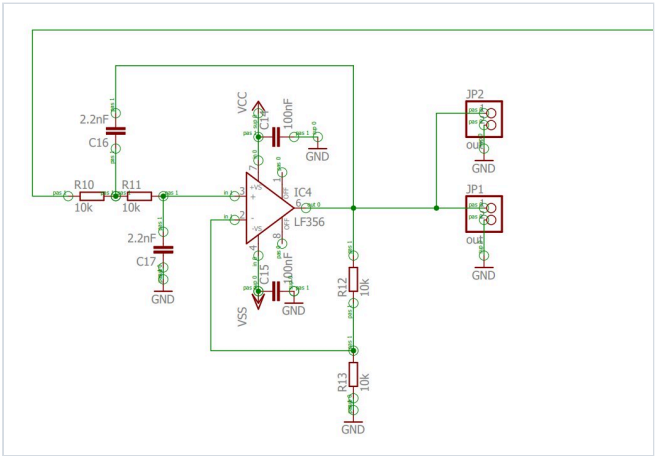


Figure 13. Active second-order low-pass (Sallen-Key) with IC4 = LF356, R10 = R11 = 10 kΩ, C16 = C17 = 2.2 nF, gain set by R12/R13.

The regenerated PWM is averaged to recover $V_{avg}(t) \approx V_0(2\alpha(t) - 1)$, the same quantity as in equation (1). With 10 kΩ and 2.2 nF the characteristic frequency is $1/(2\pi \cdot 10\ k\Omega \cdot 2.2\ nF) \approx 7.2$ kHz: well below the ~90–100 kHz switching rate and above most of the voice band. A second-order roll-off attenuates the switching fundamental by roughly $(97/7.2)^2 \approx 180$.

5 · From schematic to board: PCB design and fabrication

After the breadboard tests, I captured the receiver in EAGLE using the given topology, chose footprints for every part, placed and routed the board, ran the design-rule check, had the layout checked by the instructor, and exported it for fabrication.

- **Placement.** The photodiode-to-TIA path is kept as short as possible, because it carries the weakest signal and is the most sensitive to picked-up noise. Decoupling capacitors sit next to each IC supply pin.
- **Routing.** Two layers (top in red, bottom in blue), with wider power and ground tracks to lower their resistance and voltage drop. Signal tracks use 45° bends. At ~100 kHz this is good manufacturing practice (no acute angles that trap etchant or lift copper), not a signal-reflection issue: the tracks are far shorter than a wavelength at these frequencies.
- **Check.** DRC for clearances, shorts and drill sizes before export.

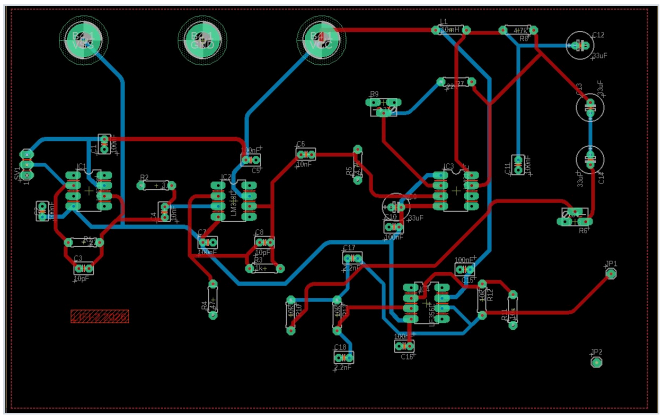


Figure 14. Two-layer layout in EAGLE.

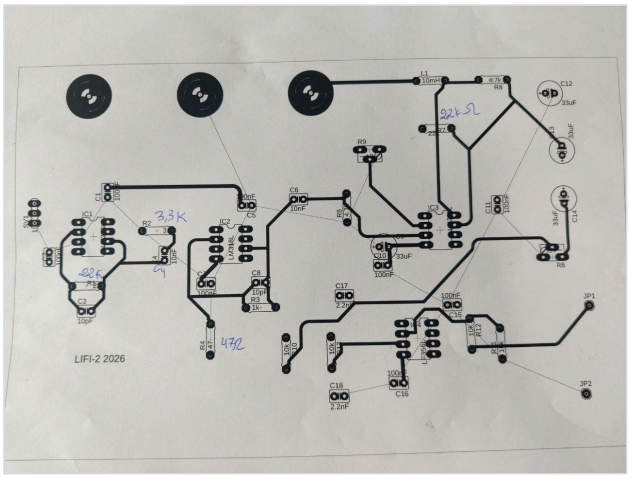


Figure 15. Printed artwork ("LIFI-2 2026") used for UV exposure.

Fabrication. UV exposure of the photosensitive board, developing, ferric-chloride etching, drilling, then soldering. Before the first power-up I checked every net for shorts and continuity, and fixed assembly faults (solder bridges, cold joints, misplaced parts) along the way. Testing then went from simple to complex: constant illumination first, then a controlled square-wave light signal from a bench function generator, so that receiver problems could be separated from transmitter behaviour.

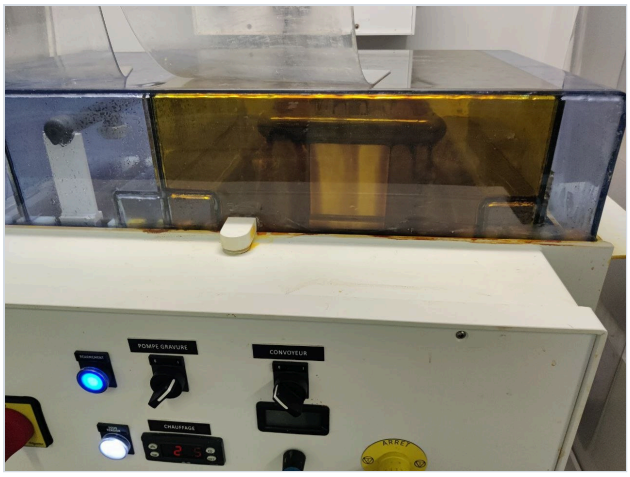


Figure 16. Etching machine used for the board.

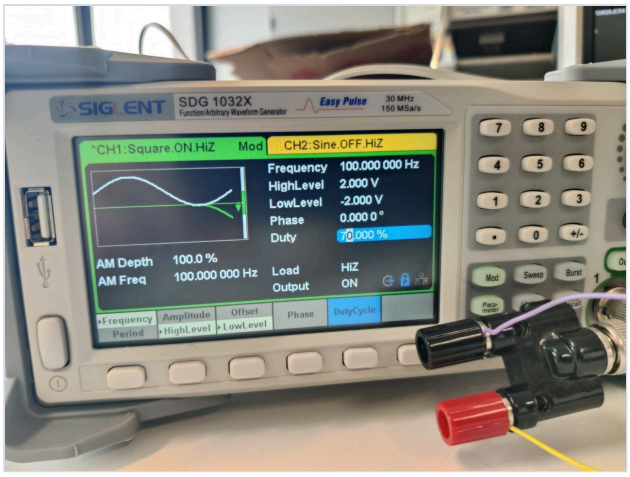


Figure 17. Bench function generator used as a known optical test source.

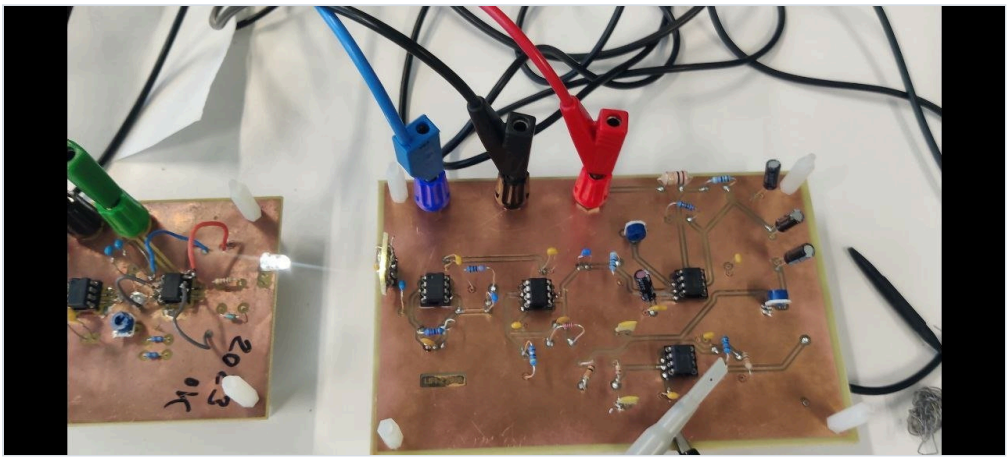


Figure 18. The finished receiver board under test, with the LED/photodiode link on the left.

6 · Receiver measurements

Static tests (constant illumination). Under steady light, the TIA output was a flat DC level of about +2 V, which is the ambient-light plus LED offset predicted by (5) and the reason Stage 2 needs a high-pass path. The comparator output stayed locked at its negative saturation level, about −4 V, because a constant input never crosses either hysteresis threshold. Both results match expectations.

Dynamic tests. The receiver was then driven by on/off light at about 97.3 kHz (frequency read by the scope). In the captures below, the purple trace is the reference square wave and the yellow trace is the probed stage. Vertical scales are printed on each screen.

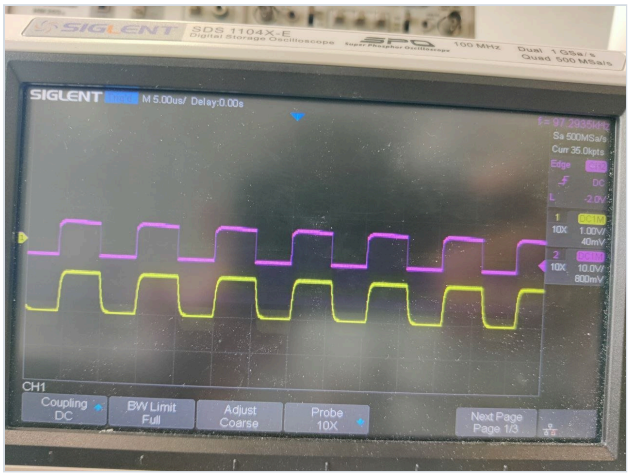


Figure 19. Stage 1, TIA output (yellow, 1 V/div): about 1 V peak-to-peak square wave with slightly rounded edges, from the finite bandwidth of the photodiode/op-amp front end.

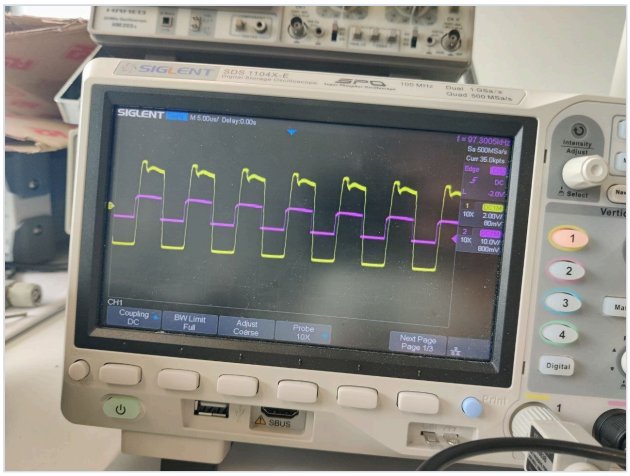


Figure 20. After conditioning (yellow, 2 V/div): amplified and recentred to about 7 V peak-to-peak. Overshoot and ringing are visible after each rising edge.



Figure 21. Stage 3, comparator output (yellow, 2 V/div, 2 µs/div): clean two-level signal with steep edges and flat plateaus, with no chatter at the transitions.

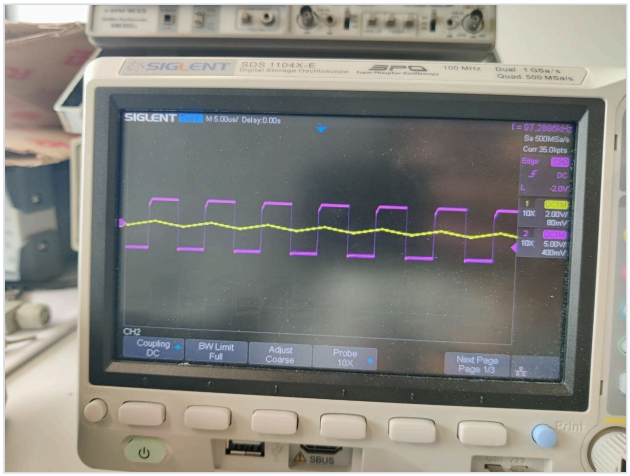


Figure 22. Low-pass (average) test point (yellow, 2 V/div): a nearly constant level with a small residual ripple at the switching rate. At constant duty cycle the average does not move.

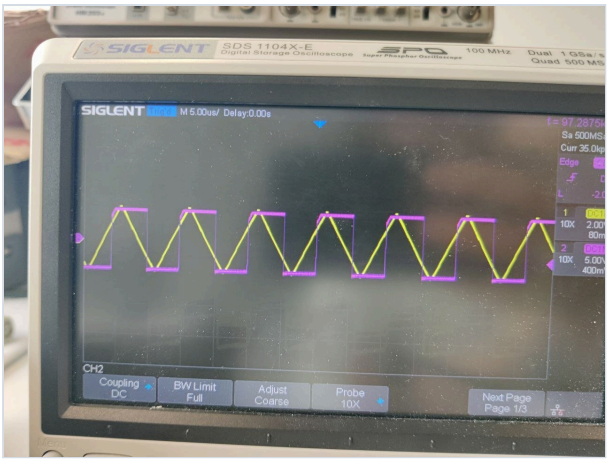


Figure 23. Reconstruction stage with a constant duty-cycle input: a regular triangle synchronized with the square wave.

With a fixed duty cycle and no audio, the filter output charges on the high states and discharges on the low states, so a triangle is the expected response, not a fault. With a real Sigma-Delta stream the duty cycle varies, and the same stage follows its slowly varying average, which is the audio.

Test point	Without signal (constant light)	With the ~97 kHz optical signal
1. TIA output	Flat DC ≈ +2 V (ambient + LED)	≈ 1 Vpp square wave on the DC offset, rounded edges
2. Conditioning output	≈ 0 V (DC removed)	≈ 7 Vpp, recentred; overshoot on rising edges
3. Comparator output	Locked at ≈ −4 V	Clean two-level square wave, sharp edges
4. Reconstruction	Constant level	Triangle at constant duty (expected); follows the average when modulated

7 · Limits and lessons

- **No end-to-end audio test on the PCB.** The receiver board was validated with a fixed-duty optical signal. The transmitter was validated separately with a 1 kHz sine. The next step is to connect both and measure the recovered tone (amplitude, distortion, signal-to-noise ratio) against distance and room light.
- **Ringing in Stage 2.** The overshoot in Figure 20 suggests limited phase margin in the conditioning amplifier, or probe/layout parasitics. The comparator hides it, but it would matter at higher data rates. Lowering the stage gain, adding a small feedback capacitor or adding a series output resistor would be the first things to try.
- **Comparator threshold.** The transmitter used three different thresholds across theory, simulation and hardware (Section 2.3). A clean redesign would fix one value and verify equation (3) on the bench.
- **Ambient-light headroom.** Brighter rooms raise the TIA offset in proportion to R_f. A DC-restoring loop or AC coupling at the photodiode would extend the usable range.

Corrections made in this edition. Compared with the French report of May 2026: the TIA op-amp is now named as on the fabricated board (LM318), and the C_f check is redone for it; the three comparator thresholds are explained rather than presented as one value; the 45° routing rule is justified as manufacturing practice, not signal reflections; oscilloscope photos have been re-captioned to describe what each screen actually

shows; a duplicated paragraph and an empty section heading were removed; the transmitter results are now checked against the charge-balance law with numbers.

What I took from it. The circuits did not behave like the ideal schematics. Ambient-light offset, the phase-margin trade-off of the TIA, ringing in a fast amplifier and the gap between simulation and the wired board only showed up once the hardware existed, with its parasitic capacitance, layout and grounding. Learning to find and explain those differences with the oscilloscope was the most useful part of the project.

8 · Conclusion

A complete optical audio link was studied, simulated and built. The Sigma-Delta transmitter self-oscillates near 87 kHz, and its duty cycle tracks the input with the slope predicted by charge balance. The LTspice study shows why coding information in time instead of amplitude makes the link robust to in-band noise. The receiver, which I laid out, fabricated, debugged and characterized, converts the photocurrent, removes the ambient-light offset, regenerates a clean two-level signal and averages it back, with each stage behaving as its analysis predicts.